DALTON
FULL PAPER

Formation of new nickel-containing nineteen-vertex metallaborane clusters prepared from the *anti*-$B_{18}H_{22}$ borane cluster: molecular structures of $[Ni(THF)_4(H_2O)_2][B_{18}H_{20}Ni(\eta^5\text{-}C_5H_5)]_2$ and $[B_{18}H_{19}(2\text{-}THF)Ni(\eta^5\text{-}C_5H_5)]$ †

Jesse W. Taylor, Ulrich Englich, Karin Ruhlandt-Senge and James T. Spencer *

Department of Chemistry and the W. M. Keck Center for Molecular Electronics, Center for Science and Technology, Syracuse University, Syracuse, New York 13244, USA

Received 12th April 2002, Accepted 19th June 2002
First published as an Advance Article on the web 8th August 2002

The reaction of the *anti*-$B_{18}H_{22}$ borane cluster with nickelocene produced several new metallaborane species, $[Ni(THF)_4(H_2O)_2][B_{18}H_{20}Ni(\eta^5\text{-}C_5H_5)]_2$ (**1a**), $[B_{18}H_{20}Ni(\eta^5\text{-}C_5H_5)]$ (**1b**) and $[N(CH_3)_4][B_{18}H_{19}(2\text{-THF})Ni(\eta^5\text{-}C_5H_5)]$ (**2**), in relatively high yields. These new complexes were fully characterized by multinuclear NMR (^1H, ^{13}C, ^{11}B), IR and UV-Vis spectroscopy. Single-crystal X-ray diffraction analyses of complexes **1a** and **2** confirmed their structures as 19-vertex *conjuncto*-metallaborane clusters. The structures consist of ten-vertex *nido*-borane subunits edge-shared with eleven-vertex *nido*-cluster subunits. In compound **2**, formed through the THF reflux of compound **1**, a THF molecule was found to coordinate at the 2-position of the borane framework.

Introduction and background

Since the late 1970's, Lipscomb and co-workers, as well as others, have predicted that larger *closo*-boranes having more than twelve vertices should be thermodynamically stable.[1] These types of clusters, however, have yet to be synthesized. The study of non-*closo* macropolyhedral borane clusters, those which have more than twelve vertices, has seen increased attention in recent years both in anticipation of their utility as synthetic precursors to larger *closo*-boranes and as models to aid in the understanding of the possible bonding and physical properties of these as yet undiscovered larger *closo*-boranes.[1] One macropolyhedral borane that has received a fair amount of study is the stable and readily synthesized *anti*-$B_{18}H_{22}$ cluster. The structure of the *anti*-$B_{18}H_{22}$ cluster consists of two 10-vertex *nido*-clusters sharing a common edge, as illustrated in Fig. 1. It has been shown that both transition metals and other hetero-atoms can be inserted into this 18-vertex *anti*-$B_{18}H_{22}$ cluster framework to obtain a variety of nineteen-vertex species.[2–5]

There are several known synthetic routes for the preparation of the *syn*- and *anti*-$B_{18}H_{22}$ cluster.[6] First reported by Hawthorne in the early 1960's, *anti*-$B_{18}H_{22}$ was initially synthesized by the acidic degradation of $[B_{20}H_{18}]^{2-}$ to $B_{18}H_{22}$.[6a] Other methods of preparation include the thermolysis of $B_9H_{13}(NHEt_2)$, the transition metal-assisted linkage of $[B_9H_{12}]^-$ by $[Os(CO)_3Cl_2]_2$, and the thermal decomposition of $B_9H_{13}S(CH_3)_2$.[7–9] An excellent preparative method for *anti*-$B_{18}H_{22}$ also involves the oxidative fusion of two $[B_9H_{12}]^-$ clusters with a mercuric halide salt and was the method employed in the work reported here.[10] Some of these synthetic methods also produce the *syn*-$B_{18}H_{22}$.[6b] The *syn*-$B_{18}H_{22}$ isomer can be seen as two *nido*-B_{10} clusters sharing the same edge (6′,7′;6,7) as shown in Fig. 1. The *anti*-$B_{18}H_{22}$ isomer, in contrast, shares adjacent edges (6′,7′;5,6) of two *nido*-B_{10} clusters, producing a centrosymmetric structure.

Sneath and Todd reported the synthesis of several nineteen-vertex metallaborane compounds based on both the *anti*- and *syn*-configurations of $B_{18}H_{22}$.[2] Compounds based on the *anti*-$B_{18}H_{22}$ isomer include nineteen-vertex transition metal species with nickel, cobalt, palladium, and rhodium incorporated into the macropolyhedral framework. These compounds were synthesized using a general pathway involving the initial deprotonation of the $B_{18}H_{22}$ cage to form the $[B_{18}H_{20}]^{2-}$ species, usually with sodium hydride, followed by reaction with a suitable organometallic reagent to produce the nineteen-vertex metallaborane, typically in yields of less than 35%. Kennedy and co-workers later reported a variety of interesting platinum derivatives of $B_{18}H_{22}$, including $[(Pt\text{-}\eta^4\text{-}anti\text{-}B_{18}H_{20})(PMe_2Ph)_2]$.[3] This platinum species was synthesized in a manner similar to that reported earlier by Todd in which the organometallic species, *cis*-$[PtCl_2(PMe_2Ph)_2]$, was reacted with *anti*-$B_{18}H_{22}$ in the presence of a base. The synthesis of the unsubstituted nineteen-vertex borane species (without hetero-

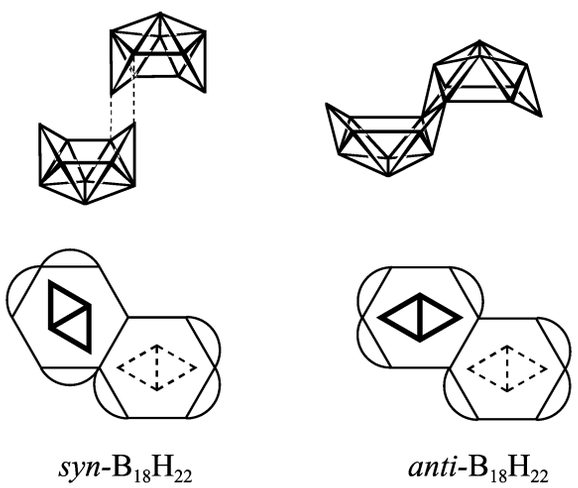

Fig. 1 The structure of *anti*-$B_{18}H_{22}$ (top) in which two *nido*-B_{10} clusters share an edge to form *anti*-$B_{18}H_{22}$ (the terminal and bridging hydrogens have been omitted for clarity). Diagrams (bottom) representing *syn*-$B_{18}H_{22}$ and *anti*-$B_{18}H_{22}$, the arcs represent bridging hydrogens.

† Electronic supplementary information (ESI) available: ^{11}B–^{11}B COSY NMR spectra for compounds **1b** and **2**. See http://www.rsc.org/suppdata/dt/b2/b203594d/

 DOI: 10.1039/b203594d

atoms), nonadecaborane, has only recently been reported.[4] Nonadecaborane has essentially the same structure as the previously described nineteen-vertex metallaboranes, with the exception that a B–H unit is inserted into the *anti*-$B_{18}H_{22}$ structure rather than an organometallic fragment. As in the previously known nineteen-vertex metallaborane species, this nonadecaborane was synthesized by deprotonation of the *anti*-$B_{18}H_{22}$ species, followed by insertion of a BH fragment through the addition of $HBCl_2{\cdot}SMe_2$. The product was obtained in a 73% overall yield. This nineteen-vertex complex is probably best formulated, however, as $[B_{19}H_{20}]^{3-}$, rather than the reported $[B_{19}H_{20}]^{-}$ species, based upon recently reported electron counting considerations.[11,12]

In this paper, we report the complete synthesis and characterization of new 19-vertex metallaboranes, $[Ni(THF)_4(H_2O)_2][B_{18}H_{20}Ni(\eta^5\text{-}C_5H_5)]_2$ (**1a**), $[N(CH_3)_4][B_{18}H_{20}Ni(\eta^5\text{-}C_5H_5)]$ (**1b**) and $[B_{18}H_{19}(2\text{-}THF)Ni(\eta^5\text{-}C_5H_5)]$ (**2**). The X-ray crystallographic characterization of compounds **1a** and **2** are also reported here.

Experimental

Physical measurements

All NMR spectra were recorded on samples in 5 mm (o.d.) tubes. The boron (^{11}B) NMR spectra were recorded on a Brüker DPX-300 NMR spectrometer operating at 96.3 MHz. Spectra were referenced to BBr_3 at +40.0 ppm (relative to $BF_3{\cdot}Et_2O$ at $\delta = 0.0$ ppm, with positive chemical shifts indicating downfield resonances). Typical ^{11}B NMR acquisition parameters employed were a relaxation delay of 0.1 ms and a 90° pulse of 10 μs. Proton (^1H) NMR spectra were recorded on a Brüker DPX-300 spectrometer operating at 300.15 MHz. Carbon (^{13}C) NMR spectra were obtained on a Brüker DPX-300 NMR spectrometer operating at 77.47 MHz. The spectrometer was operated in the FT mode while locked on the deuterium resonance of the solvent. Mass spectra were obtained in the Mass Spectrometry Laboratory, School of Chemical Sciences, University of Illinois, supported in part by a grant from the National Institute of General Medical Sciences. The 70-VSE mass spectrometer was purchased in part with a grant from the Division of Research Resources, National Institutes of Health (RR 04648). Unit resolution mass spectra were obtained on a Hewlett Packard model 5989B gas chromatograph/mass spectrometer (GC/MS) using an ionization potential of between 11 and 70 eV. Elemental analysis was performed by Complete Analysis Laboratories, Inc., E & R Microanalytical Division, Parsippany, NJ. FT-IR spectra in the range of 400 to 4000 cm^{-1} were measured on a Mattson Galaxy 2020 spectrometer and were referenced to the 1602.8 cm^{-1} band of polystyrene. UV-Vis spectral data were collected on a Cary 1 UV-Vis spectrophotometer in a quartz cell.

Materials

All solvents were reagent grade or better.Tetrahydrofuran (THF) and hexane were distilled over potassium metal prior to use. Nickelocene was sublimed prior to use. The *anti*-$B_{18}H_{22}$ was synthesized as previously described.[10] TLC plates were purchased from the Aldrich Chemical Company. All other commercially available reagents were used as received.

Synthesis

$[Ni(THF)_4(H_2O)_2][B_{18}H_{20}Ni(\eta^5\text{-}C_5H_5)]_2$ (1a) and $[(CH_3)_4N][B_{18}H_{20}Ni(\eta^5\text{-}C_5H_5)]$ (1b). In an inert atmosphere, 154 mg (0.71 mmol) of *anti*-$B_{18}H_{22}$ were placed in a dry Schlenk flask. To the borane solid was added 30 mL of dry THF. This solution was then degassed with three freeze–pump–thaw cycles. To a dry tipper tube was added 134 mg (0.71 mmol) of freshly sublimed nickelocene. This solid was added to the borane solution at room temperature quickly in one portion. The mixture was allowed to stir at room temperature for 30 minutes, during which time the reaction mixture turned a dark green color. The reaction mixture was then concentrated and diethyl ether was added to form a green oil. The solvent was decanted from the oil. Suitable crystals for a single crystal X-ray analysis of $[Ni(THF)_4(H_2O)_2][B_{18}H_{20}Ni(\eta^5\text{-}C_5H_5)]_2$ (**1a**), were grown by the slow evaporation of a saturated THF solution. **1a** was not further isolated but water was added to the remaining green oil of **1a** followed by a small amount of THF to dissolve the oil. A saturated aqueous solution of tetramethylammonium chloride was added until no more solid precipitated. The solid was filtered off, dried, and pure product $[(CH_3)_4N][B_{18}H_{20}Ni(\eta^5\text{-}C_5H_5)]$ (**1b**) was collected in 76% yield. Complete NMR (^1H, ^{11}B, and ^{13}C), IR, elemental analysis and electronic spectral data for compounds **1a** and **1b** are given in Tables 1 and 2. Crystallographic and structural data for compound **1a** are given in Tables 3 and 4.

$[B_{18}H_{19}(2\text{-}THF)Ni(\eta^5\text{-}C_5H_5)]$ (2). In an inert atmosphere, 75 mg (0.35 mmol) of *anti*-$B_{18}H_{22}$ were placed in a dry Schlenk flask. To the borane solid was added 30 mL of THF. This solution was then degassed with three freeze–pump–thaw cycles. To a dry tipper tube was added 65 mg (0.33 mmol) of freshly sublimed nickelocene. This was added quickly at room temperature to the borane solution in one portion. The reaction flask was then equipped with a reflux condenser and an oil bubbler and the reaction mixture was heated to reflux for two hours. The mixture was then cooled to room temperature and the solvent removed *in vacuo*. The remaining green residue was extracted with benzene and eluted on a silica gel column (3 cm × 30 cm) with THF as the mobile phase. The green band was collected and the solvent was removed *in vacuo*. Pure product $[B_{18}H_{19}(2\text{-}THF)Ni(\eta^5\text{-}C_5H_5)]$ (**2**) was collected in an 82% yield. Suitable crystals of **2** for single crystal X-ray analysis were grown by the slow evaporation of a concentrated THF solution. Complete NMR (^1H, ^{11}B, and ^{13}C), IR, mass and electronic spectral data for compound **2** are given in Tables 1 and 2. Crystallographic and structural data for compound **2** are given in Tables 3 and 5.

X-Ray crystallographic studies of $[Ni(THF)_4(H_2O)_2]$-$[B_{18}H_{20}Ni(\eta^5\text{-}C_5H_5)]_2$ (1a) and $[B_{18}H_{19}(2\text{-}THF)$-$Ni(\eta^5\text{-}C_5H_5)]$ (2)

Suitable crystals of compounds **1a** and **2** were selected under a microscope, attached to a glass fiber, and immediately placed in the low temperature nitrogen stream of the diffractometer.[13] All data sets were collected using a Siemens SMART system, complete with 3-circle goniometer and CCD detector operating at −54 °C. The data sets were collected at 150 K and 92 K, respectively, employing graphite monochromated Mo-Kα radiation (λ = 0.71073 Å). The data collections nominally covered a hemisphere of reciprocal space utilizing a combination of three sets of exposures, each with a different ϕ angle, and each exposure covering 0.3° in ω. Crystal decay was monitored by repeating the initial frames at the end of the data collection and analyzing the duplicate reflections. No decay was observed. An absorption correction was applied utilizing the program SADABS.[14] The crystal structures were solved by direct methods included in the SHELX program package.[15] Missing atoms were located in subsequent difference Fourier cycles and included in the refinement. The structures were refined by full-matrix least-squares refinement on F^2 (SHELXL-96).[15] All non-hydrogen atoms were refined anisotropically. All hydrogen atoms on the boron cage and in the organic ring systems were found in difference Fourier maps and refined with U_{iso} constrained at 1.2 times U_{eq} of the carrier atom. The crystallographic programs used for structure

Table 1 Multinuclear (^{11}B, ^{1}H, and ^{13}C) NMR data for compounds (**1a**), (**1b**), and (**2**)

Cmpd	^{11}B NMR [a,b] (ppm)	^{1}H{^{11}B} NMR [c] (ppm)	^{13}C NMR [d] (ppm)
1a	16.1 (s, B(18), J_{BH} = 100.3 Hz), 15.1 (s, B(12), J_{BH} = 130.8 Hz), 10.1 (s, B(2,10) unresolved), 9.1 (s, B(5) unresolved), 7.3 (s, B(3) unresolved), 6.1 (s, B(8,9,11) unresolved), 1.8 (s, B(19), J_{BH} = 153.1 Hz), 0.4 (s, B(1), J_{BH} = 139.3 Hz), −3.8 (s, B(14), J_{BH} = 124.9 Hz), −4.8 (s, B(16), J_{BH} = 103.6 Hz), −16.8 (s, B(13), J_{BH} = 154.3 Hz), −21.6 (s, B(4), J_{BH} = 141.5 Hz), −23.0 (s, B(17), J_{BH} = 136.6 Hz), −29.3 (s, B(6), J_{BH} = 141.6 Hz), −35.9 (s, B(15), J_{BH} = 145.2 Hz)	5.01 (s, η^5-C_5H_5), 4.16 (s, $B_{18}H_{20}$), 3.95 (s, $B_{18}H_{20}$), 3.62 (m, THF), 2.93 (s, $B_{18}H_{20}$), 2.63 (s, $B_{18}H_{20}$), 2.40 (s, $B_{18}H_{20}$), 1.92 (s, H_2O), 1.84 (m, THF), 1.61 (s, $B_{18}H_{20}$), 0.27 (s, $B_{18}H_{20}$), 0.08 (s, $B_{18}H_{20}$), −0.39 (s, $B_{18}H_{20}$), −0.63 (s, $B_{18}H_{20}$), −1.61 (s, $B_{18}H_{20}$), −3.08 (s, $B_{18}H_{20}$)	98.6 (s, η^5-C_5H_5), 68.7 (s, THF), 26.6 (s, THF)
1b	16.1 (s, B(18), J_{BH} = 100.3 Hz), 15.1 (s, B(12), J_{BH} = 130.8 Hz), 10.12 (s, B(2,10) unresolved), 9.1 (s, B(5) unresolved), 7.3 (s, B(3) unresolved), 6.1 (s, B(8,9,11) unresolved), 1.8 (s, B(19), J_{BH} = 153.1 Hz), 0.4 (s, B(1), J_{BH} = 139.3 Hz), −3.8 (s, B(14), J_{BH} = 124.9 Hz), −4.8 (s, B(16), J_{BH} = 103.6 Hz), −16.8 (s, B(13), J_{BH} = 154.3 Hz), −21.6 (s, B(4), J_{BH} = 141.5 Hz), −23.0 (s, B(17), J_{BH} = 136.6 Hz), −29.3 (s, B(6), J_{BH} = 141.6 Hz), −35.9 (s, B(15), J_{BH} = 145.2 Hz)	5.01 (s, η^5-C_5H_5), 4.16 (s, $B_{18}H_{20}$), 3.95 (s, $B_{18}H_{20}$), 3.09 (s, $(CH_3)_4N$), 2.93 (s, $B_{18}H_{20}$), 2.63 (s, $B_{18}H_{20}$), 2.40 (s, $B_{18}H_{20}$), 1.61 (s, $B_{18}H_{20}$), 0.27 (s, $B_{18}H_{20}$), 0.08 (s, $B_{18}H_{20}$), −0.39 (s, $B_{18}H_{20}$), −0.63 (s, $B_{18}H_{20}$), −1.61 (s, $B_{18}H_{20}$), −3.08 (s, $B_{18}H_{20}$)	98.82 (s, η^5-C_5H_5), 91.01 (s, $(CH_3)_4N$)
2	29.5 (s, B(2)), 15.7 (s, B(12,18), J_{BH} = 137.7 Hz), 9.4 (s, B(10), unresolved), 6.2 (s, B(11,5), J_{BH} = 134.5 Hz), 3.0 (s, B(19,9), J_{BH} = 154.8 Hz), 1.3 (s, B(3,8), J_{BH} = 196.2 Hz), −0.7 (s, B(1), J_{BH} = 161.1 Hz), −3.6 (s, B(14,16), J_{BH} = 134.5 Hz), −18.9 (s, B(13), J_{BH} = 154.0 Hz), −22.3 (s, B(17), J_{BH} = 144.7 Hz), −25.9 (s, B(4), J_{BH} = 147.5 Hz), −31.5 (s, B(6), J_{BH} = 144.9 Hz), −36.1 (s, B(15), J_{BH} = 150.2 Hz)	5.51 (s, η^5-C_5H_5), 4.80 (m, THF), 4.47 (s, $B_{18}H_{19}$), 3.98 (s, $B_{18}H_{19}$), 3.29 (s, $B_{18}H_{19}$), 3.16 (s, $B_{18}H_{19}$), 2.87 (s, $B_{18}H_{19}$), 2.62 (s, $B_{18}H_{19}$), 2.37 (m, THF), 1.86 (s, $B_{18}H_{19}$), 1.66 (s, $B_{18}H_{19}$), 1.38 (s, $B_{18}H_{19}$), 0.91 (s, $B_{18}H_{19}$), 0.27 (s, $B_{18}H_{19}$), 0.08 (s, $B_{18}H_{19}$), −0.22 (s, $B_{18}H_{19}$), −0.76 (s, $B_{18}H_{19}$), −1.02 (s, $B_{18}H_{19}$), −2.85 (s, $B_{18}H_{19}$)	100.07 (s, η^5-C_5H_5), 84.32 (s, THF), 31.30 (s, THF)

[a] Relative to BBr_3 (40.0 ppm). [b] Abbreviations: s = singlet. [c] Relative to $SiMe_4$ (0.0 ppm). [d] Relative to $SiMe_4$ (0.0 ppm). Abbreviations: s = singlet. [e] Solvent: CD_3CN.

Table 2 Infrared, mass spectral, elemental analysis, and electronic data for (**1a**), (**1b**), and (**2**)

Compound	IR [a]/cm^{-1}	Mass spectral data [b]/elemental analysis	Electronic spectra [c]/nm
1a and **1b**	2949(w), 2850(w), 2524(s)	Anal. Calc'd (Found) for $C_9H_{37}B_{18}Ni$ (**1b**): C, 26.18 (25.97); H, 9.03 (9.18); N, 3.39 (3.25)	215, 301,[d] 346, 436
2	2956(w), 2855(w), 2536(m)	Nominal mass: 405(found 24.1, calc'd 11.3; P^+ envelope), 406(found 37.7, calc'd 27.5; P^+ envelope), 407(found 59.9, calc'd 53.6; P^+ envelope), 408(found 86.8, calc'd 82.7; P^+ envelope), 409(found 100.0, calc'd 100.0; P^+ envelope; base peak; $^{12}C_9{}^{1}H_{32}{}^{10}B_3{}^{11}B_{15}{}^{58}Ni{}^{16}O$), 410(found 93.4, calc'd 93.2; P^+ envelope), 411(found 69.4, calc'd 67.2; P^+ envelope), 412(found 40.5, calc'd 38.7; P^+ envelope), 413(found 22.3, calc'd 19.1; P^+ envelope), 414(found 11.8, calc'd 8.3; P^+ envelope), 337(rel. int. 31.9; $P^+ - O(CH_2)_4$; $^{12}C_5{}^{1}H_{24}{}^{10}B_3{}^{11}B_{15}{}^{58}Ni$)	232, 298,[d] 346, 352, 433

[a] KBr pellet. Abbreviations; s = strong, m = moderate, w = weak, sp = sharp. [b] Relative intensities are given with the largest peak in the envelope normalized to 100.0%. The calculated values are based on the natural isotopic abundances of the elements that are normalized to the most intense peak in the envelope. [c] Solvent: CH_3CN. [d] λ_{max}/nm.

solution and refinement were installed on a PC clone and a Silicon Graphics Indigo^2 R10000 High Impact computer. Scattering factors were those provided with the SHELX program system.[15]

CCDC reference numbers 184019 and 184020.

See http://www.rsc.org/suppdata/dt/b2/b203594d/ for crystallographic data in CIF or other electronic format.

Results and discussion

A new transition metal derivative of *anti*-$B_{18}H_{22}$, $[Ni(THF)_4(H_2O)_2][B_{18}H_{20}Ni(\eta^5\text{-}C_5H_5)]_2$ (**1a**), was synthesized by the reaction of *anti*-$B_{18}H_{22}$ with freshly sublimed nickelocene in THF. In order to avoid THF substitution on the boron cage (*vide infra*) it was necessary to maintain this reaction at room temperature for less than 30 min. The nickel dication counterion was readily exchanged with $[(CH_3)_4N]^+$ to produce $[(CH_3)_4N][B_{18}H_{20}Ni(\eta^5\text{-}C_5H_5)]$ (**1b**). The ^{11}B and ^{1}H NMR of both compounds **1a** and **1b** are essentially identical, supporting the notion that the structures of the two compounds are very similar. The ^{11}B NMR data of both **1a** and **1b** are also quite similar to the data previously reported for several other nineteen-vertex boranes and metallaboranes.[2,3,5] Typically, compounds with the nineteen-vertex *conjuncto*-metallaborane structure display five signals (B(4), B(6), B(13), B(15), and B(17)) in the region of −17 ppm to −36 ppm in the ^{11}B{^{1}H} NMR. When the organometallic fragment is inserted into the *anti*-$B_{18}H_{22}$ cluster, the centrosymmetric symmetry of the structure is lost. This generates the five observed signals from three original signals in the *anti*-$B_{18}H_{22}$ cluster. These five peaks actually consist of overlapping resonances from neighboring signals which arise from the symmetry lowering caused by the

Table 3 Crystallographic data for (**1a**) and (**2**)

	1a	**2**
Empirical formula	$C_{42}H_{118}B_{36}Ni_3O_6$	$C_9H_{32}B_{18}NiO$
M	1284.19	413.67
Crystal system	Triclinic	Monoclinic
Space group	$P\bar{1}$	$P2(1)/n$
a/Å	12.1061(3)	7.45170(10)
b/Å	12.7869(3)	19.9456(2)
c/Å	13.6348(2)	14.9108(2)
α/°	115.2020(10)	90
β/°	98.9130(10)	98.3280(10)
γ/°	99.04(1)	90
V/Å^3	1827.01(7)	2192.80(5)
Z	1	4
λ/Å	0.71073	0.71073
T/K	150(2)	92(2)
ρ_{calc}/g cm^{-3}	1.226	1.253
μ/mm^{-1}	0.812	0.884
2*θ* range/°	3.40 to 56.44	3.44 to 56.54
No. of reflections collected	11631	17943
No. of reflections with [$I > 2\sigma(I)$]	7945	5224
No. of parameters	496	345
Final *R* indices	$R1 = 0.0604$, $wR2 = 0.1601$	$R1 = 0.0294$, $wR2 = 0.0616$
Largest diff. peak and hole (e Å^{-3})	1.685 and −1.121	0.256 and −0.251

Table 4 Selected interatomic distances (Å) and angles (°) for $[Ni(THF)_4(H_2O)_2][B_{18}H_{20}Ni(\eta^5\text{-}C_5H_5)]_2$ (**1a**)

Ni(7)–C(1)	2.079(3)	Ni(7)–B(2)	2.068(4)
Ni(7)–C(2)	2.090(3)	Ni(7)–B(3)	2.062(4)
Ni(7)–C(3)	2.203(3)	Ni(7)–B(11)	2.184(3)
Ni(7)–C(4)	2.159(3)	B(10)–B(11)	1.850(5)
Ni(7)–C(5)	2.090(4)	B(8)–H(8B)	1.42(5)
Ni(7)–B(8)	2.158(4)	B(9)–H(8B)	1.34(5)
B(2)–Ni(7)–B(8)	49.72(14)	B(11)–Ni(7)–B(8)	93.47(13)
B(3)–Ni(7)–B(8)	90.28(14)	B(9)–B(10)–B(11)	111.8(2)
Ni(7)–B(11)–B(10)	111.5(2)	Ni(7)–B(8)–B(9)	114.9(2)
B(8)–B(9)–B(10)	107.7(2)	B(16)–B(17)–B(10)	115.1(3)

Table 5 Selected interatomic distances (Å) and angles (°) for $[B_{18}H_{19}\text{-}(2\text{-}THF)Ni(\eta^5\text{-}C_5H_5)]$ (**2**)

Ni(7)–C(1)	2.0778(15)	Ni(7)–B(2)	2.0267(15)
Ni(7)–C(2)	2.0911(14)	Ni(7)–B(3)	2.0528(15)
Ni(7)–C(3)	2.0976(14)	Ni(7)–B(11)	2.1981(16)
Ni(7)–C(4)	2.1927(15)	B(10)–B(11)	1.843(2)
Ni(7)–C(5)	2.1270(15)	B(10)–B(17)	1.842(2)
Ni(7)–B(8)	2.1342(16)	B(2)–O(1)	1.5163(17)
B(2)–Ni(7)–B(8)	50.20(6)	B(11)–Ni(7)–B(8)	93.98(6)
B(3)–Ni(7)–B(8)	90.86(6)	B(9)–B(10)–B(11)	110.42(11)
Ni(7)–B(11)–B(10)	111.77(9)	Ni(7)–B(8)–B(9)	114.57(9)
B(8)–B(9)–B(10)	108.55(11)	B(16)–B(17)–B(10)	115.48(12)
B(2)–O(1)–C(6)	117.0(4)	B(2)–O(1)–C(9)	124.7(4)

organometallic framework substitution. Two of the three original *anti*-$B_{18}H_{22}$ signals in this upfield region are split into four signals; two signals from the half of the cluster that remains essentially unchanged, B(13) and B(15), and two signals from the half of the cluster that contains the new organometallic moiety, B(4) and B(6). The ^{11}B NMR spectra for compounds **1a** and **1b** display fifteen resonances. The complete unambiguous assignment of the ^{11}B NMR signals to specific boron atoms in these compounds was accomplished from ^{11}B–^{11}B COSY NMR experiments.

Both the IR data, including the B–H stretch at 2524 cm^{-1}, and the elemental analysis data (Table 2) for compounds **1a** and **1b** are consistent with a compound having a nineteen-vertex *conjuncto*-structure. The UV-Vis spectrum for **1b** consists of four bands at 215, 301, 346, and 436 nm. The three higher energy bands arise from the cage subunit, being slightly red-shifted from *anti*-$B_{18}H_{22}$ (218, 271, and 329 nm).[16] The band at 436 nm is most likely a charge transfer band involving the Ni(η^5-C_5H_5) fragment.

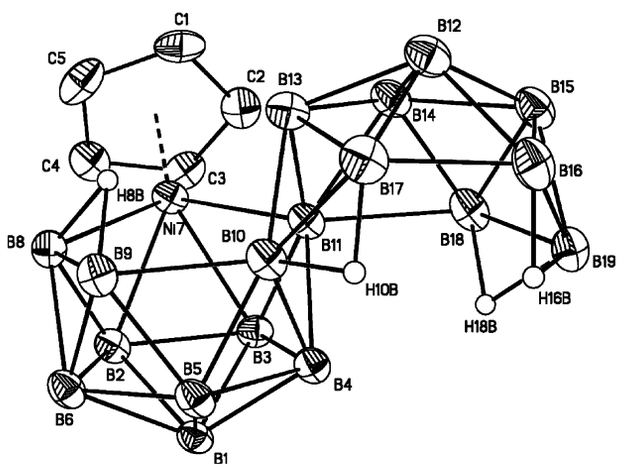

Fig. 2 Crystallographically determined structure of $[Ni(THF)_4(H_2O)_2][B_{18}H_{20}Ni(\eta^5\text{-}C_5H_5)]_2$ (**1a**), with thermal ellipsoids drawn at the 30% probability level. The nickel dication and terminal hydrogens have been omitted for clarity.

Suitable crystals of **1a** were grown from the slow evaporation of a THF solution of the compound. The molecular structure of the anion of $[B_{18}H_{20}Ni(\eta^5\text{-}C_5H_5)]_2$ (**1a**) is shown in Fig. 2. This structure was found to be quite similar to the other structurally known nineteen-vertex boranes and metallaboranes, $[(Ph_3P)_2N][B_{19}H_{20}]$ and $[B_{18}H_{20}Pt(PhMe_2P)_2]$.[3,4] The overall structure of **1a** consists of a *nido*-10-vertex cluster subunit sharing an edge with a *nido*-11-vertex cluster subunit. Selected bond distances and angles are given Table 4. While there are several other examples of this type of nineteen-vertex cluster compound, few have reported crystallographic structures. Schematic drawings of the known boranes and metallaboranes are shown in Fig. 3, in which the similarities between these previously reported compounds and the new compounds reported here can be seen. The X-ray crystal structure of [Pt-η^4-*anti*-$B_{18}H_{20}(PMe_2Ph)_2$] and the nineteen-vertex borane, nonadecaborane, have been reported.[3,4] In compound **1a**, the Ni–B bonds are in the range of 2.062 Å to 2.184 Å. In the Pt–B_{18} compound, the Pt–B bonds are longer, 2.24 Å to 2.36 Å, due to the larger size of the platinum atom.[3] For nonadecaborane, the boron–boron bond lengths of the original B_{18}-subunit to the newly inserted boron atom are in the range of 1.744 Å to 1.907 Å.[4] These distances are overall shorter than the

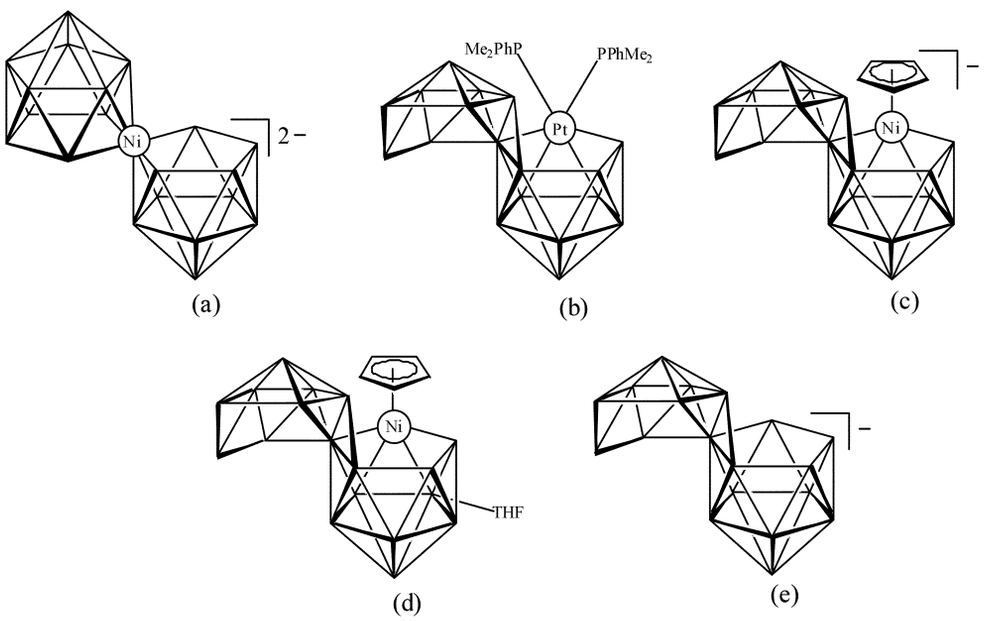

Fig. 3 Schematic drawings of various boranes and metallaboranes; (a) $[Ni(B_{10}H_{12})_2]^{2-}$, (b) [Pt-$\eta^4$-*anti*-$B_{18}H_{20}(PMe_2Ph)_2$], (c) $[B_{18}H_{20}Ni(\eta^5\text{-}C_5H_5)]^-$, (**1a**) (d) $[B_{18}H_{19}(2\text{-THF})Ni(\eta^5\text{-}C_5H_5)]$, (**2**) (e) $[B_{19}H_{20}]^{(1\text{ or }3)-}$.

reported organometallic inserted B_{18}-clusters, due principally to the relative size of the boron atom compared with the metal atoms. There is also a known NiB_{10} complex that exhibits a *nido*-11-vertex structure similar to the metal-inserted portion of **1a**. This known compound, $[(CH_3)_4N]_2[Ni(B_{10}H_{12})_2]$, consists of two *nido*-11-vertex clusters that share a common vertex, the nickel atom.[17] In this compound, the Ni–B bond lengths are in the range of 2.11 Å to 2.24 Å, which are very similar to those observed for compound **1a**.

Another 19-vertex borane cluster, $[B_{18}H_{19}(2\text{-THF})Ni(\eta^5\text{-}C_5H_5)]$ (**2**), was also synthesized by altering the reaction conditions that had been used to prepare $[Ni(THF)_4(H_2O)_2][B_{18}H_{20}Ni(\eta^5\text{-}C_5H_5)]_2$ (**1a**). Freshly sublimed nickelocene was reacted with *anti*-$B_{18}H_{22}$ in refluxing THF for two hours. An unidentified oxidizing agent is generated in a side reaction which oxidizes **1a**, allowing for the coordination of a THF molecule to the cluster to produce $[B_{18}H_{19}(2\text{-THF})Ni(\eta^5\text{-}C_5H_5)]$ (**2**). Similar oxidation and ether substitution has previously been seen to occur in other metallaborane species, such as the oxidation of $[6\text{-}(CO)_3\text{-}6\text{-}MnB_9H_{13}]^-$ with $HgCl_2$ in the presence of THF to form $[2\text{-THF-}6\text{-}(CO)_3\text{-}6\text{-}MnB_9H_{12}]$.[18] Alternatively, the cluster could be self-oxidizing through the necessary removal of the two hydrogens from $B_{18}H_{22}$ to form complex **1a**. The ^{11}B NMR spectrum of **2** is quite similar to that observed for **1a** and **1b**, with the exception that the resonance for the THF-substituted boron shifts approximately 19 ppm downfield from its original position in compound **1**. The $^{11}B\{^1H\}$ NMR spectra of compounds **1b** and **2** are shown in Fig. 4, where the chemical shift for the boron in the 2-position has moved from 10.1 ppm in the **1b** cluster to 29.5 ppm in compound **2**. This 19 ppm downfield shift is typical for THF substitution in borane cluster compounds and several examples from the literature show similar ^{11}B NMR shifts upon THF substitution.[18,19] These shifts can be as small as 15 ppm downfield in the case of a THF-substituted diborane[18] or as large as 28 ppm downfield in the THF-substituted metallanonaborane, $[2\text{-THF-}6(CO)_3\text{-}6\text{-}MnB_9H_{12}]$.[19] The ^{11}B–^{11}B COSY NMR of compound **2** allowed for the complete assignment of the boron atoms in the ^{11}B spectrum.

The IR and UV-Vis data for compound **2** are also quite similar to those observed for compounds **1a** and **1b** and both are consistent with data for other previously known nineteen-vertex metallaboranes. The mass spectral analysis for **2** also provides further confirmation for the proposed composition

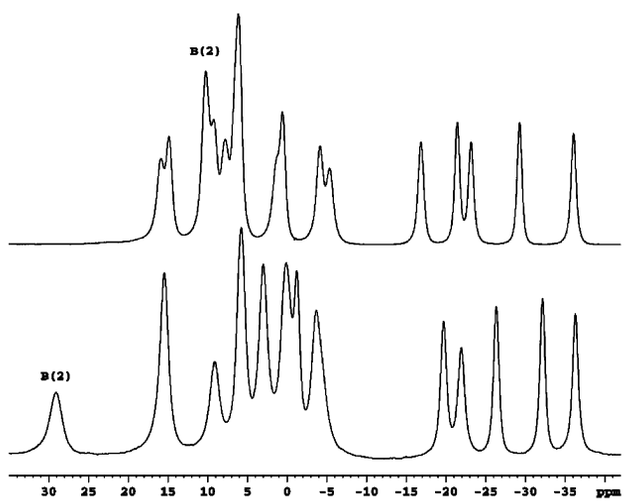

Fig. 4 The $^{11}B\{^1H\}$ NMR of $[(CH_3)_4N][B_{18}H_{20}Ni(\eta^5\text{-}C_5H_5)]$ (**1b**) (top), and $[B_{18}H_{19}(2\text{-THF})Ni(\eta^5\text{-}C_5H_5)]$ (**2**), (bottom).

with the base peak, which is also the parent ion peak, at 409 u. There is also a fragment peak at 337 u that originates from the parent ion peak minus a THF molecule. The UV-Vis spectrum of **2** is essentially identical to the unsubstituted species **1a** and **1b** (Table 2).

The X-ray crystal structure of this new product, $[B_{18}H_{19}(2\text{-THF})Ni(\eta^5\text{-}C_5H_5)]$ (**2**), shows it to have a similar structure to the other previously reported nineteen-vertex cluster structures (Fig. 5). Selected bond distances and angles for **2** are given in Table 5. The Ni–B bond lengths in compound **2** range from 2.027 Å to 2.198 Å. These are almost identical to the distances found in the unsubstituted cluster **1a**. The THF ring in compound **2** is, however, disordered. These similarities are expected due to the overall similarities of compounds **1a** and **2**.

These new compounds have structures fully consistent with recently reported electron counting schemes for *conjuncto*-cluster species.[11,12] For example, the new 19-vertex species $[B_{18}H_{20}Ni(\eta^5\text{-}C_5H_5)]^-$ (**1a** and **1b**), consists of two edge-fused clusters incorporating a $[Ni(\eta^5\text{-}C_5H_5)]$ subunit, four bridging hydrogens and an overall 1− charge. Using this reported counting scheme requires this cluster to contain twenty-three electron pairs (19 vertices + 2 subunits + 2 open faces = 23 electron

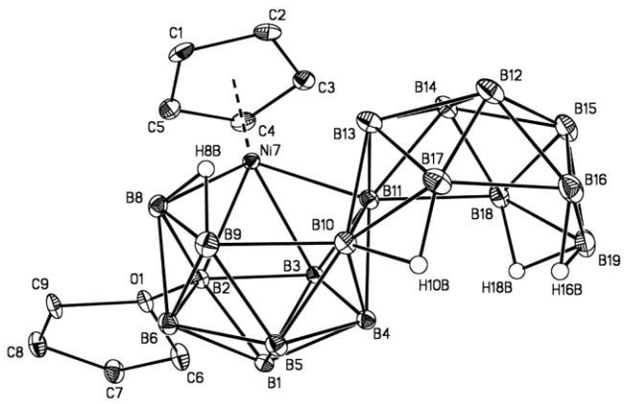

Fig. 5 Crystallographically determined structure of $[B_{18}H_{19}(2\text{-}THF)Ni(\eta^5\text{-}C_5H_5)]$ (**2**), with thermal ellipsoids drawn at the 30 % probability level. The terminal hydrogens have been removed for clarity.

pairs). The observed structure derives 16 pairs from the 16 BH units, 1.5 pairs from the $[Ni(\eta^5\text{-}C_5H_5)]$ subunit (a 3 electron cage donor which is isolobal with the BH^- fragment), three pairs from the two *conjuncto*-B atoms, two pairs from the four bridging hydrogen atoms, and 0.5 pairs from the net 1− charge, yielding a total of the required twenty-three electron pairs.

Conclusions

From this work it can be seen that there still remains a vast amount of chemistry with the stable and easily synthesized *anti*-$B_{18}H_{22}$ compound. We have shown that new 19-vertex metallaborane species can be readily synthesized in reasonable yields and that this chemistry should be able to be expanded to include many other organometallic–borane clusters.

Acknowledgements

We are grateful to Sandy Kotiah and Jonathan Melnick for their assistance with portions of the synthetic work. We are grateful to Dr Deborah Kerwood for her assistance with obtaining the NMR data reported here. Finally, we wish to thank the National Science Foundation and the Donors of the Petroleum Research Fund for their generous support of this work (PRF35284-AC3). Also, we wish to thank the National Science Foundation (grant CHE-9527898), Syracuse University, and the W. M. Keck Foundation for the purchase of the X-ray instrument and computers.

References

1 L. D. Brown and W. N. Lipscomb, *Inorg. Chem.*, 1977, **16**, 2989; M. L. McKee, Z.-X. Wang and P. Ragu von Schleyer, *J. Am. Chem. Soc.*, 2000, **122**, 4781.
2 R. L. Sneath and L. J. Todd, *Inorg. Chem.*, 1973, **12**, 44.
3 Y. M. Cheek, N. N. Greenwood, J. D. Kennedy and W. S. McDonald, *J. Chem. Soc., Chem. Commun.*, 1982, 80.
4 J. A. Dopke, D. R. Powell and D. F. Gaines, *Inorg. Chem.*, 2000, **39**, 463.
5 J. W. Taylor, U. Englich, K. Ruhlandt-Senge and J. T. Spencer, *Inorg. Chem. Commun.*, 2002, **5**, 274.
6 (*a*) A. R. Pitochelli and M. F. Hawthorne, *J. Am. Chem. Soc.*, 1962, **84**, 3218; (*b*) F. P. Olsen, R. C. Vasavada and M. F. Hawthorne, *J. Am. Chem. Soc.*, 1968, **90**, 3846.
7 F. Meyer, U. Englert and P. Paetzold, *Chem. Ber.*, 1994, **127**, 853.
8 J. Bould, N. N. Greenwood and J. D. Kennedy, *Polyhedron*, 1983, **2**, 1401.
9 J. Plesek, S. Hermanek, B. Stibr and F. Hanousek, *Collect. Czech. Chem. Commun.*, 1967, **32**, 1095.
10 D. F. Gaines, C. K. Nelson and snf G. A. Steehler, *J. Am. Chem. Soc.*, 1984, **106**, 7266.
11 E. D. Jemmis, M. M. Balakrishnarajan and P. D. Pancharatna, *Inorg. Chem.*, 2001, **40**, 1730.
12 E. D. Jemmis, M. M. Balakrishnarajan and P. D. Pancharatna, *J. Am. Chem. Soc.*, 2001, **123**, 4312.
13 H. Hope, *Prog. Inorg. Chem.*, 1994, **41**, 1.
14 G. M. Sheldrick, Program for absorption correction using area detector data, University of Gottingen, Germany, 1996.
15 SHELXTL-Plus, A program package for the solution and refinement of crystal structure, Bruker Analytical X-ray Systems, Madison, WI, 1997.
16 F. P. Olsen, R. C. Vasavada and M. F. Hawthorne, *J. Am. Chem. Soc.*, 1968, **90**, 3946.
17 L. J. Guggenverger, *J. Am. Chem. Soc.*, 1972, **94**, 114.
18 G. R. Eaton and W. N. Lipscomb, *NMR Studies of Boron Hydrides and Related Compounds*, W. A. Benjamin, New York, NY, 1969.
19 J. W. Lott and D. F. Gaines, *Inorg. Chem.*, 1974, **13**, 2261.